REPORT DOCUMENTATION PAGE

Form Approved
OMB No. 0704-0188

AD-A264 710

2. REPORT DATE	3. REPORT TYPE AND DATES COVERED
March 1993	Professional Paper

4. TITLE AND SUBTITLE

SIMULTANEOUS DISORDERING AND ISOLATION INDUCED BY ION MIXING IN InGaAs/InP SUPERLATTICE STRUCTURES

5. FUNDING NUMBERS

PR: EE04
PE: 0601153N
WU: DN587579

6. AUTHOR(S)

S. A. Pappert, W. Xia, B. Zhu, A. R. Clawson, Z. F. Guan, P. K. L. Yu, S. S. Lau

7. PERFORMING ORGANIZATION NAME(S) AND ADDRESS(ES)

Naval Command, Control and Ocean Surveillance Center (NCCOSC)
RDT&E Division
San Diego, CA 92152–5001

8. PERFORMING ORGANIZATION REPORT NUMBER

9. SPONSORING/MONITORING AGENCY NAME(S) AND ADDRESS(ES)

Office of Naval Research
800 North Quincy Street
Arlington, VA 22217

10. SPONSORING/MONITORING AGENCY REPORT NUMBER

11. SUPPLEMENTARY NOTES

12a. DISTRIBUTION/AVAILABILITY STATEMENT

Approved for public release; distribution is unlimited.

12b. DISTRIBUTION CODE

13. ABSTRACT *(Maximum 200 words)*

The phenomenon of simultaneous compositional disordering and the formation of electrical resistive layers induced by oxygen implantation in InGaAs/InP superlattices has been investigated. The disordering characteristics have been studied as a function of implantation temperature and ion dose. It was found that implantation at elevated temperatures (referred to as the IM or ion mixing process) usually leads to much more efficient disordering compared to implantation at room temperature followed by annealing at the same elevated temperature (referred to as the implantation plus annealing process). Of particular interest is the observation that ion mixing at 550 °C with 1×10^{13} O^+/cm@ leads to significantly more disordering than implantation with the same dose at room temperature followed by annealing at 550 °C for the same period of ion mixing time. In addition, the electrical resistance of the ion-mixed layer at 550 °C increases 2600 times for the *p*-type InGaAs/InP superlattice structure, whereas the sample implanted at room temperature and annealed at 550 °C showed only a 20 times increase in electrical resistance. These results indicate a distinct advantage for the IM process in achieving simultaneous compositional disordering and electrical isolation for optoelectronic applications.

Published in Applied Physic Letter 61(11), Vol. 72, No. 4, Aug 1992, pp 1306–13..

14. SUBJECT TERMS

electro-optics; Quantum wells; electronic devices, components, and subsystems; infrared sensors; INGAAS/INP

15. NUMBER OF PAGES

16. PRICE CODE

17. SECURITY CLASSIFICATION OF REPORT	18. SECURITY CLASSIFICATION OF THIS PAGE	19. SECURITY CLASSIFICATION OF ABSTRACT	20. LIMITATION OF ABSTRACT
UNCLASSIFIED	UNCLASSIFIED	UNCLASSIFIED	SAME AS REPORT

21a NAME OF RESPONSIBLE INDIVIDUAL	21b TELEPHONE *(include Area Code)*	21c OFFICE SYMBOL
S. A. Pappert	(619) 553-5704	Code 555

Simultaneous disordering and isolation induced by ion mixing in InGaAs/InP superlattice structures

S. A. Piccpert,[a] W. Xia, B. Zhu, A. R. Clawson, Z. F. Guan, P. K. L. Yu, and S. S. Lau
Department of Electrical and Computer Engineering, University of California at San Diego, La Jolla, California 92093-0407

(Received 24 February 1992; accepted for publication 30 April 1992)

The phenomenon of simultaneous compositional disordering and the formation of electrical resistive layers induced by oxygen implantation in InGaAs/InP superlattices has been investigated. The disordering characteristics have been studied as a function of implantation temperature and ion dose. It was found that implantation at elevated temperatures (referred to as the IM or ion mixing process) usually leads to much more efficient disordering compared to implantation at room temperature followed by annealing at the same elevated temperature (referred to as the implantation plus annealing process). Of particular interest is the observation that ion mixing at 550 °C with 1×10^{13} O^+/cm^2 leads to significantly more disordering than implantation with the same dose at room temperature followed by annealing at 550 °C for the same period of ion mixing time. In addition, the electrical resistance of the ion-mixed layer at 550 °C increases 2600 times for the *p*-type InGaAs/InP superlattice structure, whereas the sample implanted at room temperature and annealed at 550 °C showed only a 20 times increase in electrical resistance. These results indicate a distinct advantage for the IM process in achieving simultaneous compositional disordering and electrical isolation for optoelectronic applications.

I. INTRODUCTION

Compositional disordering of III-V compound superlattice structures has received considerable attention recently due to its potential application for photonic devices.[1] A commonly used method to induce compositional disordering in a layered structure is to implant a moderate dose ($\sim10^{15}/cm^2$) of shallow dopant ions (e.g., Si for *n*-type and Zn for *p*-type) into the structure at room temperature, followed by a high-temperature annealing step [this process is referred to as implantation plus annealing (IA) here].[2–15] Ion irradiation at room temperature alone with light mass ions (e.g., O, Si, or Ar) does not cause significant intermixing of layers; the subsequent high-temperature annealing is needed to cause disordering and the annealing of implantation damage, but this step tends to restrict device processing flexibility. Ion mixing (IM) is capable of enhancing compositional disordering of layers at a rate which increases exponentially with the ion irradiation temperature above a critical temperature. The critical temperature, T_c, is system dependent for III-V superlattice structures.[16] As a processing technique to planarize devices, ion mixing appears to be an attractive technology.

In optoelectronics and electronics, device isolation is an important issue. Highly resistive regions can be created by implanting H, He, O, Cr, and Fe ions into the III-V material of interest.[17] For *p*-type InGaAs/InP superlattices, it appears that oxygen ions may be a good choice for simultaneous compositional disordering and the creation of highly resistive regions using the ion mixing process. This is based on the consideration that oxygen is a deep donor and has a significant atomic mass (compared to H and He) to induce ion mixing and yet light enough (compared to Fe) to have a deep ion range into the material using a 200 kV implanter. We have previously reported that ion mixing with Ar ions is useful in fabricating planar waveguides in InGaAs/InP quantum well structures.[18] In this work, our objectives are to study the ion mixing phenomena in InGaAs/InP superlattice structures for simultaneous compositional disordering and the formation of highly resistive regions. The IA process will also be investigated for these effects in comparison with the IM process.

II. EXPERIMENT

The InGaAs/InP superlattice structures investigated here were grown by low pressure metalorganic chemical vapor deposition (LP-MOCVD) which has been described elsewhere.[19] Nominally lattice-matched $In_{0.53}Ga_{0.47}As$/InP superlattices consisting of 50 periods of 20 Å InGaAs wells and 80 Å InP barriers were grown on undoped and semi-insulating InP substrates. Undoped and Zn doped *p*-type 20 Å/80 Å superlattice structures were grown with the top layer being a 200-Å-thick InGaAs layer.

Ion implantations were performed at temperatures ranging from LN_2 to 550 °C. Oxygen ions were chosen for ion mixing in order to simultaneously achieve compositional disordering and electrical isolation of *p*-type superlattices. Oxygen ions (O^+) were implanted into the superlattice structures at an energy of 180 keV and an incident angle of 7° with respect to the sample surface normal. For each implant, half the sample was shielded from the ion beam to allow the monitoring of any thermally induced changes to the as-grown superlattice. Penetration depths of $R_p\approx3650$ Å, $\Delta R_p\approx1380$ Å, are projected from this O^+

[a] Also with the Naval Command, Control and Ocean Surveillance Center, RDT&E Division, San Diego, CA 92152.

 0021-8979/92/161306-06$04.00

implantation. Implantation doses ranging from 5×10^{12}/cm^2 to 5×10^{14}/cm^2 were used. To maximize thermal conductivity between the samples and the sample stage, the samples were mounted on the heating and cooling stage with indium. For the 550 °C annealing, samples implanted at low temperatures were mounted on the heating stage but shielded from the ion beam while the ion mixing was directly performed at 550 °C on another sample so that the annealing and ion mixing conditions were very similar. The 650 °C annealings were carried out in a rapid thermal annealing system with samples facing a Si substrate in a flowing forming gas (15% H_2, 85% N_2) ambient. The samples were examined using x-ray diffraction, photoluminescence (PL), absorption, and surface resistance measurements.

III. RESULTS AND DISCUSSION

The temperature dependence of the ion mixing behavior of the InGaAs/InP material system has been investigated. The InGaAs (20 Å)/InP (80 Å) superlattice structures was implanted with 1×10^{13} O$^+$/cm^2 at four different temperatures; LN_2, room temperature (RT), 200 °C, and 550 °C. This implantation dose was determined to be sufficient for nearly complete compositional disordering within the resolution limits of the x-ray diffraction measurement. The integration time was 5 s with the Bartels x-ray diffractometer.[20] For direct comparison, the samples implanted at LN_2, RT, and 200 °C were annealed at 550 °C for 8 min which corresponded to the 550 °C implant duration. X-ray rocking curves (XRCs) were used to measure the degree of disordering exhibited by each sample. The XRC for the as-grown superlattice structure is shown in Fig. 1(a). Well-resolved satellite peaks indicative of high-quality epitaxial growth are present. The sharp peak at 0° is the InP substrate peak and the zero order peak of the superlattice is slightly lattice mismatched. XRCs of the four implanted samples are shown in Figs. 1(b)–1(e). It is here found that the 550 °C implanted sample shown in Fig. 1(e) does exhibit the lowest satellite peak levels. It is difficult to quantitatively measure the degree of mixing although the 550 °C implanted sample definitely shows the most mixing while the 200 °C implanted sample shown in Fig. 1(d) displays the least mixing. These results are not surprising and will now be discussed.

It has previously been shown that the ion mixing process is a diffusion-like process where the ion dose, ϕ, can be considered to be equivalent to the diffusion time, t, in diffusion.[16] In this case, the decay of the normalized x-ray intensity is related to an effective diffusion coefficient for ion mixing by the following equation:[16]

$$\frac{d}{d\phi}\ln\left(\frac{I}{I_0}\right)=-KD, \tag{1}$$

where I_0 is the normalized intensity before mixing, I is the normalized intensity after mixing, K is a constant, and D is the effective diffusion coefficient. The conventional diffusion length, $(Dt)^{1/2}$, can be replaced by $(D\phi)^{1/2}$. A plot of $\ln(I/I_0)$ vs ϕ yields a straight line with a slope proportional to the value of D at a given ion mixing temperature.

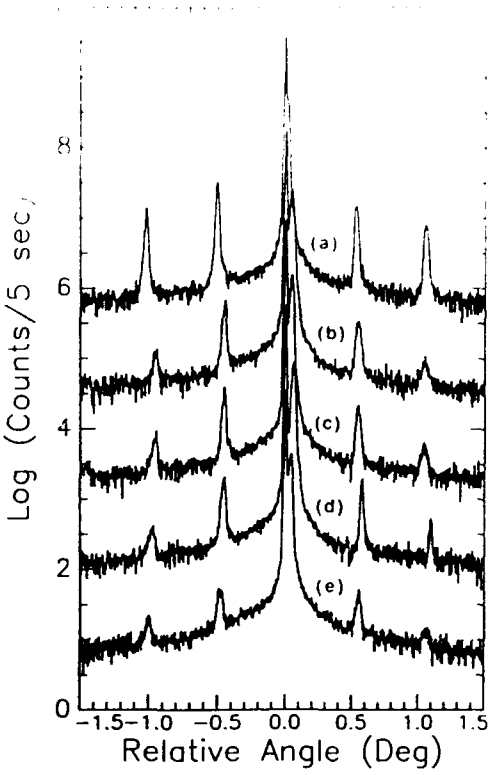

FIG. 1. X-ray rocking curves for a 50 period $In_{0.53}Ga_{0.47}As$ (20 Å)/InP (80 Å) superlattice before (a) and with 1×10^{13} O$^+$ cm^2 ions at 180 keV at (b) LN_2 temperature, (c) room temperature, (d) 200 °C, and (e) 550 °C. Samples b, c, and d were annealed at 550 °C for 8 min after ion irradiation. The annealing time was the same as the implantation time for sample e which was implanted at 550 °C. The XRC indicated that sample e was more disordered than all other samples. The (400) reflection was used here.

The temperature dependence of Ar ion mixing for the InGaAs/InP system is shown in Fig. 2. The mixing rate is taken to be the term KD shown in Eq. (1) and is plotted in Fig. 2 with arbitrary units. It can be seen that ion mixing rates are quite temperature independent below the critical temperature, T_c, of about 185 °C and the rates increase exponentially above T_c with an activation energy of about 0.24 eV. While the temperature dependent behavior of mixing shown in Fig. 2 was obtained for Ar ions, the general characteristics of this behavior remain relatively unchanged for oxygen and other ions with a significant mass.[16,21] Based on the much enhanced mixing rates in the thermally activated regime of ion mixing and that shallow dopant atoms are not needed for efficient mixing, it was deemed possible to achieve simultaneous compositional disordering and the formation of highly resistive regions by oxygen ion mixing at moderately elevated temperatures to allow for a self-aligned process.

Referring back to the temperature dependent XRC results, implantation below $T_c\sim185$ °C should result in significantly less disordering than that of high temperature implants. Implantation below about 185 °C, where there is no thermal enhancement of the mixing process, the disordering is relatively temperature independent. Mixing below T_c is essentially due to the freezing-in or storing of defects

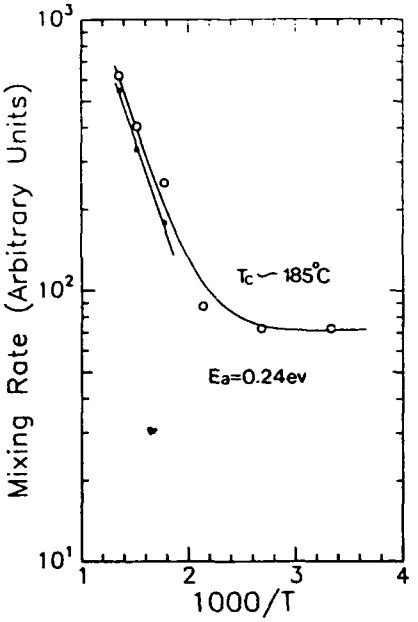

FIG. 2. Ion mixing rate vs $1/T$ for InGaAs/InP samples implanted with Ar^+ (190 keV) ions. The solid symbols represent the net mixing rates, i.e., subtracting the rate below T_c from that above T_c.

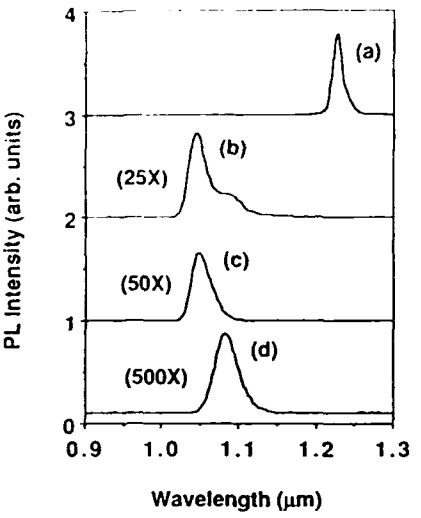

FIG. 3. Photoluminescence spectra of a 50 period InGaAs (20 Å)/InP (80 Å) superlattice for (a) the as-grown sample, (b) the sample implanted with 1×10^{13} O^+/cm^2 at 550 °C, (c) the sample implanted with 1×10^{13} O^+/cm^2 at room temperature followed by annealing at 550 °C for 8 min and 650 °C for 15 min, and (d) the sample implanted with 5×10^{14} O^+/cm^2 at room temperature followed by annealing at 550 °C for 8 min and 650 °C for 15 min.

in the structure which can contribute to the mixing process under subsequent annealing. It follows that the more defects that can be stored in the structure, the more mixing can occur provided voids and clusters do not form due to over-implantation.[22] One would expect more stored defects with decreasing implantation temperatures. The XRC results shown in Fig. 1 suggest that this is indeed the case as the LN_2 implant displays slightly more mixing than the RT implant which displays still more mixing than the 200 °C implant upon annealing at 550 °C. Implantation close to T_c results in the least efficient mixing. At this temperature, both the high temperature IM advantages and the low temperature stored defect advantages are minimized. Further, the XRC results imply that the 550 °C IM process does have an advantage over the IA process with a post implant annealing temperature of 550 °C in terms of mixing efficiency.

Low temperature PL has also been used to examine the four oxygen implanted samples. The PL spectrum of the as-grown superlattice taken at a sample temperature of ~20 K is shown in Fig. 3(a). A multiline argon ion laser with an estimated incident optical intensity of 0.5 W/cm^2 was used to obtain this spectrum. The PL peak near 1.22 μm is due to the lowest order InGaAs(20 Å)/InP(80 Å) superlattice transition and has a full width at half maximum (FWHM) linewidth of 12 meV. PL spectra of the four implanted samples were obtained and energy blue shifts of 118, 124, 95, and 175 meV have been measured for the samples implanted at LN_2, RT, 200 °C, and 550 °C, respectively. Again, the samples implanted at temperatures less than 550 °C have been annealed at 550 °C for 8 min which corresponds to the 550 °C implant duration. The PL spectrum of the sample implanted at 550 °C is shown in Fig. 3(b) and displays the most PL energy shift while the sample implanted at 200 °C displays the least energy shift which is consistent with the XRC results of most and least mixed samples, respectively. The PL peak of the sample implanted at 550 °C displays a FWHM linewidth of 32 meV. The cause of the long wavelength side shoulder of this PL peak is not clear at this time. Assuming a fully mixed alloy, $In_{0.9}Ga_{0.1}As_{0.2}P_{0.8}$, an energy blue shift of 265 meV is expected. From the PL measurement, this implies the sample implanted at 550 °C as well as the other implanted samples are not completely disordered. This is also consistent with the XRC results which showed measurable satellite peaks after implantation. As a result, subsequent annealing of the four implanted samples at 650 °C for 15 min was performed in an attempt to mix the samples further. After annealing at 650 °C, the PL energy shift of the LN_2, RT, and 550 °C implanted samples increased to 160, 170, and 178 meV, respectively. A significant increase in the PL energy shift upon 650 °C annealing was found for the samples implanted at RT and LN_2 temperature. This was not the case for the sample implanted at 550 °C as the 650 °C post implantation annealing only increased the PL energy shift by 3 meV. The sample implanted at 200 °C exhibited only a 130 meV PL energy shift with 650 °C annealing which further indicates the disadvantage of implanting near T_c. Table I summarizes the actual PL energy shifts incurred by each of the four implanted samples. The XRC results of the 650 °C annealed samples implanted at LN_2, RT, 200 °C, and 550 °C were consistent with the PL results and satellite peaks were still observable on each of the four samples. Longer 650 °C anneals to 30 min of the four implanted samples resulted in no further PL energy shifts.

The disordering efficiency of both the IA and IM pro-

TABLE I Summary of PL energy shifts for a 50 period InGaAs(20 Å)/InP(80 Å) superlattice structure with various implantation and annealing conditions.

Anneal conditions \ Implant temperature and dose (O^+/cm^2)	1×10^{13} (LN_2)	1×10^{13} (RT)	5×10^{14} (RT)	1×10^{13} (200 °C)	1×10^{13} (550 °C)	5×10^{14} (550 °C)
Sample at 550 °C for 8 min	118 meV	124 meV	...[a]	95 meV	175 meV	...[a]
Additional anneal at 650 °C for 15 min	160 meV	170 meV	134 meV	130 meV	178 meV	195 meV

[a]... means no observable PL signal.

cesses at different implantation doses has also been investigated. Implants performed at RT and 550 °C at doses of 1×10^{13} O^+/cm^2 and 5×10^{14} O^+/cm^2 were annealed for 15 min at 650 °C followed by PL and XRC measurements. The PL data for the 1×10^{13} O^+/cm^2 implants were given above where 170 and 178 meV PL energy shifts were obtained for both the RT and 550 °C implanted samples, respectively. The PL spectra for the samples implanted at RT with 1×10^{13} O^+/cm^2 and 5×10^{14} O^+/cm^2 and annealed at 650 °C are shown in Figs. 3(c) and 3(d), respectively. A PL energy shift of only 134 meV with a FWHM linewidth of 37 meV was obtained for the sample implanted at RT with 5×10^{14} O^+/cm^2 and subsequent 650 °C annealing. A PL energy shift of 195 meV with a FWHM linewidth of 32 meV was obtained for the sample implanted at 550 °C with 5×10^{14} O^+/cm^2 and subsequent 650 °C annealing. These results compared to those obtained for implants with 1×10^{13} O^+/cm^2 suggest that a higher implantation dose does not always lead to more disordering in the case of IA. High implantation doses at RT can lead to the formation of voids or clusters upon annealing which do not contribute to the mixing processes.[21] This is evidently the case here in that a lower implantation dose results in a larger PL energy shift and hence, more mixing. For the IA process, maximum disordering should be obtained for an implantation dose just below the dose required to form voids upon annealing. For the IM process, higher implantation doses should lead to larger PL energy shifts and hence, more mixing. Voids and clusters are not expected to form readily under high temperature implantation which should result in more mixing as implied by Eq. (1). This is indeed the case as the sample implanted at 550 °C with 5×10^{14} O^+/cm^2 followed by annealing at 650 °C for 15 min displays a 17 meV larger PL energy shift as that observed for the sample implanted with 1×10^{13} O^+/cm^2 followed by annealing at 650 °C for 15 min (see Table I). An XRC measurement of the sample implanted at 550 °C with 5×10^{14} O^+/cm^2 followed by a 15 min 650 °C anneal showed no observable satellite peaks. This is consistent with the PL result of more mixing for this sample compared to that of the sample implanted at 550 °C with 1×10^{13} O^+/cm^2 followed by a 650 °C anneal for 15 min (see Table I).

To be most useful in optoelectronic device technology, one desires this implantation process to modify the refractive index of the superlattice material as well as the conductivity. The refractive index change due to implantation can be deduced from the change in material absorption. The absorption spectra of the as-grown superlattice and the sample implanted at 550 °C with 1×10^{13} O^+/cm^2 are shown in Figs. 4(a) and 4(b), respectively. It is here seen that the absorption coefficient for the two curves differ significantly only in the 1.0–1.4 μm optical wavelength range. Performing a Kramers–Kronig transformation[23] on the change in absorption coefficient spectrum, an index of refraction change of approximately -0.07% or -2% is incurred at an optical wavelength of 1.5 μm, an important wavelength for optoelectronic device applications. This refractive index change is enough to cause lateral confinement and to produce optical channel waveguides with planar structures. Less index change was obtained for samples implanted at LN_2, RT, and 200 °C followed by annealing at 550 °C. These results further indicate the advantage of the IM process.

For integration and device compatibility issues, the electrical isolation properties of this implantation process are also important. Before and after implant resistance measurements were obtained on the samples implanted at RT and 550 °C with 1×10^{13} O^+/cm^2. The samples were processed as follows: ohmic metallization was deposited

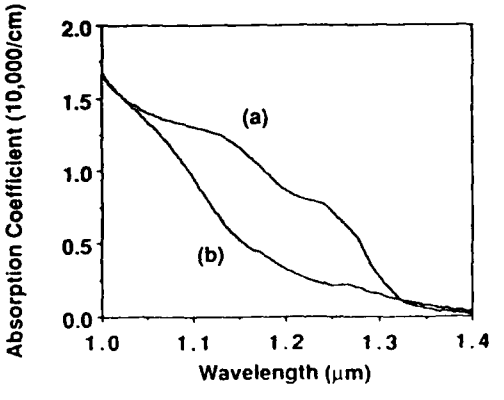

FIG. 4. Absorption spectrum of a 50 period InGaAs(20 Å)/InP(80 Å) superlattice without (a) and with (b) 1×10^{13} O^+/cm^2 550 °C implant

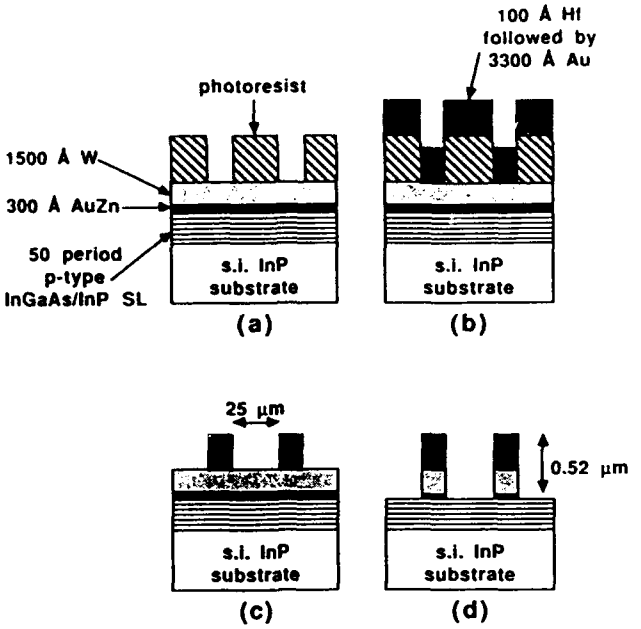

FIG. 5. Metallization processing steps used in preparing the 50 period InGaAs (20 Å)/InP(80 Å) *p*-type superlattice for ion implantation and subsequent resistance measurements. The steps include (a) metal deposition for ohmic contact (AuZn) and diffusion barrier (W) followed by photolithography, (b) metal deposition for adhesion (Hf) and ion mask (Au), (c) liftoff of the photoresist, and (d) chemical etching of the W and AuZn layers.

first on the *p*-type InGaAs/InP superlattice using a layer of evaporated AuZn (300 Å) followed by a layer of rf sputtered W (1500 Å). Photolithography was used to open contact pad windows 25 μm in separation. An *e*-beam evaporated 100 Å layer of Hf followed by 3300 Å of Au was then deposited on the sample and liftoff was performed leaving the Hf/Au structure in the contact window area. The W and the AuZn layers outside of the contact areas were etched off using the contact pads as etching masks. The processing steps for metallization are summarized in Figs. 5(a)–5(d). The metallization structure was designed such that the AuZn layer is used for ohmic contact, the W layer is used as a diffusion barrier, the Hf for adhesion purposes, and the Au as a final ion mask. The samples were then implanted using the metal layers as self-aligned ion masks. The ohmic contact was made during ion mixing or post annealing at 550 °C. Upon implantation at 1×10^{13} O^+/cm^2, the *p*-type superlattice surface resistance increased from 300 Ω to 6 kΩ for the sample implanted at room temperature (RT) followed by annealing at 550 °C for 8 min and from 300 Ω to 794 kΩ for the sample ion mixed at 550 °C. This corresponds to a 20 times and 2600 times increase in the surface resistance for the 550 °C IA and IM processes, respectively. It is not clear whether the large increase in surface resistance for the IM process is due to electronic compensation or damage induced traps. More work is required to clarify these results. Nonetheless, a big advantage in device isolation characteristics has been observed for the 550 °C IM process over the 550 °C IA process which should allow for self-aligned, planar guided-wave optoelectronic devices to be produced. Fabrication of guided-wave InP based devices using ion-mixing induced compositional disordering techniques are in progress in our laboratory and will be reported at a later time.

IV. CONCLUSION

Compositional disordering of *p*-type InGaAs/InP superlattices using oxygen ion implantation has been investigated. Both elevated temperature implantation (IM) and room temperature implantation followed by annealing (IA) have been studied by XRC, PL, and surface resistance measurements. It has been shown that oxygen is a good candidate for ion mixing of InGaAs/InP superlattices to promote layer intermixing and provide isolation. The results indicate that the 550 °C IM process is far superior to the 550 °C IA process in terms of both mixing efficiency and device isolation properties. The results further suggest that the 550 °C IM process is useful in developing a self-aligned device fabrication process. For processing other than at 550 °C, IM followed by additional annealing is still superior to IA followed by additional annealing due to the lower tendency to form voids upon implantation at elevated temperature. In summary, our results suggest that for the case of *p*-type InGaAs/InP superlattices, oxygen ion mixing is a valuable tool for producing compositionally disordered and highly resistance layers.

ACKNOWLEDGMENTS

The financial support of NSF, DARPA (A. Yang), and ONR (Y. S. Park) are gratefully acknowledged.

[1] For a review, see D. Deppe and N. Holonyak, Jr., J. Appl. Phys. **64**, R93 (1988).
[2] E. A. Dobisz, B. Tell, H. G. Craighead, and M. C. Tamargo, J. Appl. Phys. **60**, 4150 (1986).
[3] P. Gavrilovic, K. Meehan, L. J. Guido, N. Holonyak, Jr., V. Eu, M. Feng, and R. D. Burnham, Appl. Phys. Lett. **47**, 130 (1985).
[4] J. J. Coleman, P. D. Dapkus, C. G. Kirkpatrick, M. D. Camras, and N. Holonyak, Jr., Appl. Phys. Lett. **40**, 904 (1982).
[5] K. B. Kahen, G. Rajeswaran, and S. T. Lee, Appl. Phys. Lett. **53**, 1635 (1988).
[6] S. T. Lee, S. Chen, G. Rajeswaran, G. Braunstein, P. Fellinger, and J. Madathil, Appl. Phys. Lett. **54**, 1145 (1989).
[7] P. M. Petroff, X. Qian, P. O. Itoltz, R. J. Simes, J. H. English, J. Merz, and R. Kubena, Mater. Res. Soc. Symp. Proc. **126**, 55 (1988).
[8] T. Venkatesan, S. A. Schwarz, D. M. Hwang, R. Bhat, H. W. Yoon, and Y. Arakawa, Nucl. Instrum. Methods Res. B **19/20**, 777 (1987).
[9] P. M. Petroff, Mater. Res. Soc. Symp. Proc. **104**, 595 (1988).
[10] P. Mei, H. W. Yoon, T. Venkatesan, S. A. Schwarz, and J. P. Harbison, Appl. Phys. Lett. **50**, 1823 (1987).
[11] H. Leier, A. Forchel, G. Hörcher, J. Hommel, S. Bayer, H. Rothfritz, G. Weimann, and W. Schlapp, J. Appl. Phys. **67**, 1805 (1990).
[12] C. Vieu, M. Schneider, R. Planel, H. Launois, B. Descouts, and Y. Gao, J. Appl. Phys. **70**, 1433 (1991).
[13] F. Xiong, T. A. Tombrello, H. Wang, T. R. Chen, H. Z. Chen, H. Morkoc, and A. Yariv, Appl. Phys. Lett. **54**, 730 (1989).
[14] E. P. Zucker, A. Hashimoto, T. Fukunaga, and N. Watanabe, Appl. Phys. Lett. **54**, 564 (1989).
[15] S. A. Schwarz, T. Venkatesan, R. Bhat, M. Koza, H. W. Yoon, Y. Arakawa, and P. Mei, Mater. Res. Soc. Symp. Proc. **56**, 321 (1986).
[16] W. Xia, S. A. Pappert, B. Zhu, A. R. Clawson, P. K. L. Yu, S. S. Lau, D. B. Poker, C. W. White, and S. A. Schwarz, J. Appl. Phys. **71**, 2602 (1992).
[17] S. J. Pearton, Mater. Sci. Rep. **4**, 313 (1990).

[18] W. Xia, S. C. Lin, S. A. Pappert, C. A. Hewett, M. Fernandes, T. T. Vu, P. K. L. Yu, and S. S. Lau, Appl. Phys. Lett. 55, 2020 (1989).
[19] A. R. Clawson and C. M. Hanson, J. Electron. Mater. 20, 365 (1991).
[20] W. J. Bartels, J. Vac. Sci. Technol. B 1, 338 (1983).
[21] B. Y. Tsaur, Ph.D. thesis, California Institute of Technology, 1980.
[22] S. Chen, S.-Tong Lee, G. Braunstein, K. Y. Ko, and T. Y. Tan, J. Appl Phys. 70, 25 (1991).
[23] J. I. Pankove, *Optical Processes in Semiconductors* (Prentice-Hall, Englewood Cliffs, NJ, 1971), Chap. 18.